Journal Pre-proof

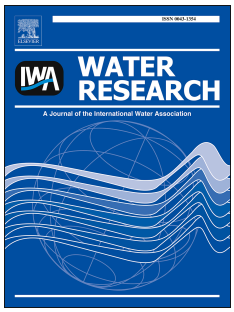

Response of bacterial community in composition and function to the various DOM at river confluences in the urban area

Yi Li, Chen Xu, Wenlong Zhang, Li Lin, Longfei Wang, Lihua Niu, Huanjun Zhang, Peifang Wang, Chao Wang

PII: S0043-1354(19)31067-X

DOI: https://doi.org/10.1016/j.watres.2019.115293

Reference: WR 115293

To appear in: *Water Research*

Received Date: 1 July 2019

Revised Date: 20 October 2019

Accepted Date: 6 November 2019

Please cite this article as: Li, Y., Xu, C., Zhang, W., Lin, L., Wang, L., Niu, L., Zhang, H., Wang, P., Wang, C., Response of bacterial community in composition and function to the various DOM at river confluences in the urban area, *Water Research* (2019), doi: https://doi.org/10.1016/j.watres.2019.115293.

Graphical Abstract:

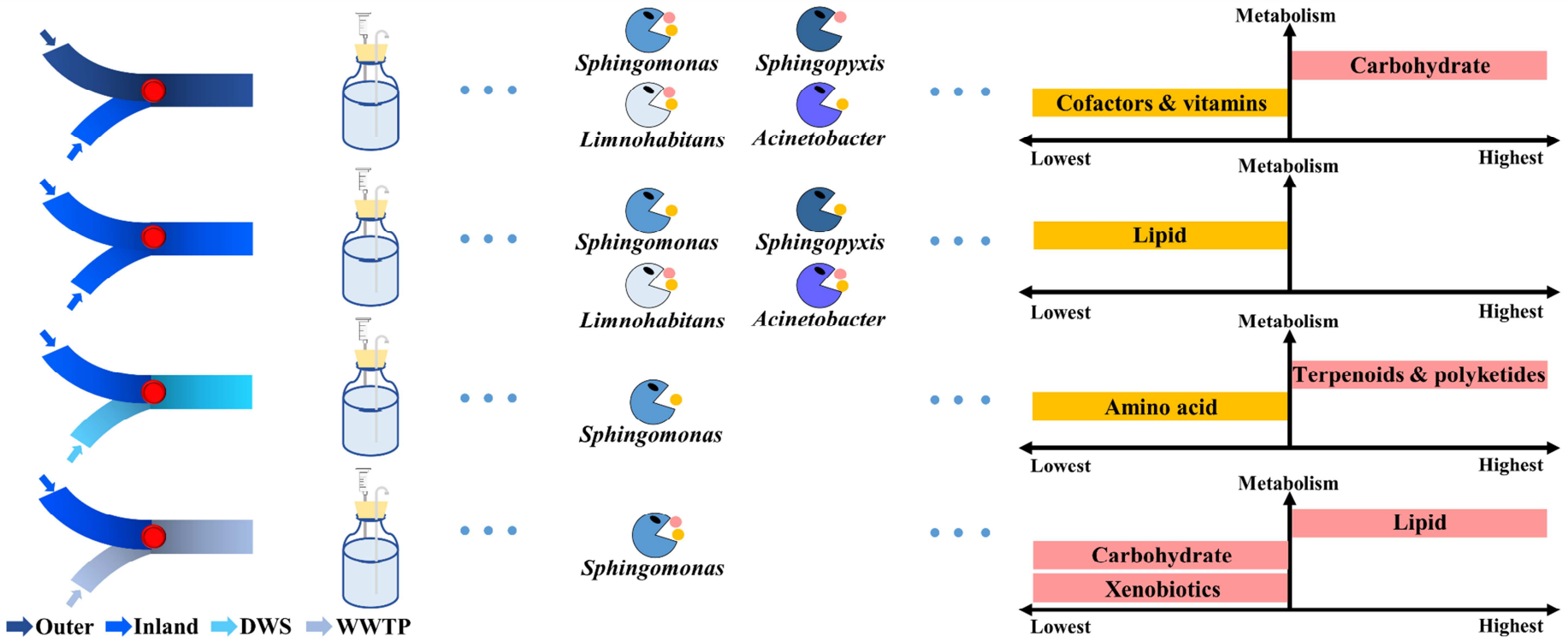

Response of bacterial community in composition and function to the various DOM at river confluences in the urban area

Yi Li[a], Chen Xu[a], Wenlong Zhang[a]*, Li Lin[b], Longfei Wang[a], Lihua Niu[a], Huanjun Zhang[a], Peifang Wang[a], Chao Wang[a]

[a] Key Laboratory of Integrated Regulation and Resource Development of Shallow Lakes, Ministry of Education, College of Environment, Hohai University, Xikang Road #1, Nanjing 210098, P.R. China

[b] Basin Water Environmental Research Department, Changjiang River Scientific Research Institute, Wuhan 430010, P.R. China

* Corresponding author:

Wenlong Zhang

College of Environment

Hohai University

Xikang Road #1, Nanjing, 210098,

P.R.China

Tel: +86 02583786696

Fax: 86-25-83786696

E-mail: 1223zhangwenlong@163.com

Abstract

River confluences result in mixture and transformation of dissolved organic matter (DOM), influencing the phylogeny of microbial community, furthermore, the integrity and function of river systems. The relationship between the microbial community and DOM is complex, especially in the confluence zone. Previous reports focused on shifts in the different bacterial community in response to exposure to the same terrestrial DOM. However, the transformation of bacterial community induced by convergent DOM remains unknown. This study showed the shifts of DOM components at the junction via excitation–emission matrices parallel factor analysis. Metabolic differences were also determined via phylogenetic investigation of communities by reconstruction of unobserved states. The results demonstrated a direct link between the microbial metabolism and DOM biodegradation during the heterotrophic process. In response to diverse DOM conditions, the taxonomic composition and metabolic function of the microbial community presented significant differences. Different taxa may be involved in metabolizing various DOM components. As indicative bacteria that are closely associated with DOM components, Proteobacteria (*Sphingomonas*) were significant for microbial utilization and were important during the DOM-degrading process. Compared with other conditions, the abundance of carbon metabolism was higher in convergences where urban rivers joined with estuary or source water. Furthermore, humic-like DOM, converging in the confluence zone, induced a more active lipid metabolism. This study applied techniques that capture the diversity and complexity of bacterial communities and

DOM, and provides new insight on the basis of the interaction between bacterial communities and DOM in confluence processes of biogeochemical significance.

Keywords: river confluence; dissolved organic matter; microbial community; functional prediction; maximal information coefficient analysis; co-occurrence

1. Introduction

River channel confluences form important geomorphological nodes in riverine networks that exert important ecological and morphological functions (Richards 1980; Rice 2017). The environmental heterogeneity, biological diversity, and productivity may peak at river confluences (Benda et al., 2004), since a number of microbes may leverage the unique hydrologic characteristics (Gualtieri et al., 2017). In the river ecosystem, dissolved organic matter (DOM), which is composed of proteinaceous substances, carbohydrates, and humic-like material, is a potentially important substrate. It supports the heterotrophic microbial metabolism (Stedmon et al., 2011) and affects both integrity and function of river ecosystems to a certain extent. Changes in the abundance and type of DOM occur in the confluence zone (Xu et al., 2018). Bound with a broad diversity of elements, such as Co, Cr, Ag, and Ni, DOM affect the chemical reactions and toxicity of trace metals in the confluences (Du et al., 2019). Moreover, the availability of highly concentrated DOM forms an important contribution to eutrophication (Guenther and Valentin 2009). Information about the dynamic changes of DOM in this process is thus of considerable importance for an improved understanding of the biogeochemical activity of the confluence zone (Xu et al., 2018).

Despite significant research pointing out that climatic, hydrogeological, and nutritional conditions in the tributaries may impact the degradation of DOM downstream (Grinsted et al., 2013; Guo et al., 2014; Zhou et al., 2016), few studies have investigated inland river confluence areas (Saarenheimo et al., 2017; Zhou et al.,

2017). However, DOM of different quality and quantity exist in multifarious water confluences such as river-lake interaction (Kaartokallio et al., 2016), in which, process biodegradation of DOM hold an important position. Import flows add a mixture of nutrients at different levels that can cause changes of the microbial community. Microbial community structure and function can shift with changing carbon loading (Traving et al., 2017). During the metabolic process, DOM character can influence water safety and ecosystem functional variables, including light absorption, nutrient cycling, pollution transport and the allochthonous microbial communities' structure and function (Beier et al., 2015). It remains unclear how the characteristic of various composed DOM will influence the microbial community and thus the fate of carbon and nutrients in the river ecosystem.

DOM cycling in the aquatic food web is decomposed by the bacteria community, and the relationship between both is complicated and bidirectional (Jansson et al., 2007). It has been reported that DOM can influence the dynamics of the major representative species of the heterotrophic bacterial community, and these groups can also participate in the DOM hydrolysis process (Kirchman et al., 2004). Aquatic settings of similar DOM concentration and character may support/engender different bacterial community structures (Logue et al., 2016). Researchers have pointed out that functionally distinct bacterial groups play key roles in the variation of bacterial respiration and production when faced with changes in DOM quality and quantity (Kirchman et al., 2004). So far, many studies have reported notable results and disciplines, e.g., the DOM degrading rules and relative changing patterns of the

bacteria community (Landa et al., 2014). However, it is difficult to find high correspondence between these. Furthermore, using phylogenetic information only derived from 16S rRNA genes to predict the DOM-utilizing ability of one taxa is still not easy (Logue et al., 2016). Due to the complex nature and various sources, DOM of exactly the same quality and composition cannot be included in two different water areas, even in similar environments (Holland et al., 2018). The associations between the response of autochthonous communities in composition and function induced by various DOM and the corresponding patterns in DOM turnover are barely known.

This study assessed structural and metabolic variations of the microbial community, the shifts in concentration and composition of DOM, and the associations of theses change at the confluence. An indoor experiment was designed in which different DOM media were inoculated with the same microbial communities. To obtain a variety of DOM characteristics over broad ranges in river confluence conditions, DOM were sampled at the intersections where urban rivers met the estuary, the drinking water source, and the effluent of wastewater treatment plant (WWTP). These areas span large gradients of environmental properties. The microbial communities were analyzed via high-throughput 16S rRNA gene sequencing and phylogenetic investigation of communities by reconstruction of unobserved states (PICRUSt) while the DOM were characterized via excitation–emission matrices parallel factor analysis (EEM-PARAFAC) analyses to determine component differences. This work contributes to the completion of the research on links between microbe utilization and DOM biodegradation based on a previous study (Logue et al.,

2016). The results provide insight into microcosmic changes of river confluence.

2. Materials and methods

2.1 Sampling

Four typical confluence areas were studied in this experiment, which are all situated in the Qinhuai River Basin of Nanjing, China (Table S1). These areas differ in dissolved organic carbon (DOC) characteristics and the types of confluent rivers. They were, respectively, an estuary (SCE) in which the Qinhuai River joined the Yangtze River, a junction (QHR), where city inland rivers converge, a site (DWS) where the drinking water source met the urban river, and the convergence (JXZ), where the effluent from a WWTP was discharged into the river.

Sampling was conducted on 22 May 2018. The confluence represented an important input of upstream freshwater and organic carbon to the downstream area. Thirty water samples (each 50 L) were taken from each site. Specific water chemistry analyses were conducted *in situ*, such as temperature, redox potential, conductivity, and DO. 1-L water samples were acid fixed and transported to the laboratory at 4 °C for further chemical analyses including TN, TP, and DOC. All samples were taking grab samples and were collected in sterile 25-L polypropylene bottles. Samples were kept cold and in the dark during transportation to the laboratory. Upon arrival at the laboratory, samples were stored at 4 °C and in the dark until further processing.

2.2 Experimental design

A batch culture approach was applied in which different media were inoculated with the same bacteria from the YR sample (Table S1). A control treatment consisted of medium made by ultrapure water, and was run alongside the four experimental treatments. Microbial inocula were added in 1-L glass bottles by precombusted GF/D filters (Guo et al., 2014), which were sealed according to (Logue et al., 2016). Batch cultures were filled without headspace and were continuously oscillated by shaker throughout the experiment.

The media were prepared from water samples collected from the four pools (SCE, QHR, DWS, and JXZ). By filtering through a 0.22-μm PES-filtrate which was rinsed with Milli-Q and heat-sterilized at 120 °C before utilization, 1-L liquid media were prepared, which were diluted to a final concentration of 17 mg C l^{-1}. Nitrogen and phosphorus were added as NH_4–NO_3 (final concentration: 8.5 mg N l^{-1}) and NaH_2–PO_4 (final concentration: 0.3 mg P l^{-1}), respectively, thus avoiding nitrogen and phosphorus limitation. Sterile media were prepared via UV (Hijnen et al., 2006).

All experimental treatments and the control were run in three independent triplicates each. The experiment was operated in a constant temperature shaker at 15 °C and in the dark. DOM fluorescence and microbial analysis were sampled nine times (at 0, 12, 24, 48, 72, 96, 120, 168, and 360 h).

2.3 Fluorescence characterization

Excitation–emission matrices (EEMs) were collected with a fluorescence spectrophotometer (F7000, Hitachi, Japan), using a 1-cm quartz cuvette. Both excitation wavelengths (λEx) and emission wavelengths (λEm) ranged from 200 to 600 nm in 5-nm increments and the integration time was 0.1 s. Blank subtraction, removal of the inner filter effects along with the 1st and 2nd order Rayleigh and Raman scatter, and calibration to Raman units was conducted, following the methods reported by previous studies (Zepp et al., 2004; Lakowicz 2013). 135 EEM samples were identified for individual fluorescing components via parallel factor analysis (PARAFAC) using the DOMFluor toolbox (Stedmon and Bro 2008) for MATLAB and Statistics Toolbox (R2017a).

2.4 DNA extraction and pyrosequencing

Microbial community compositions were assessed via next generation sequencing of the 16S rRNA gene. Samples (500 ml) for DNA extraction were filtered onto separate 0.22-mm cellulose-acetate filters (Gelman Supor R). DNA was extracted using the FastDNA spin kit for soil (Q-BIOgene, Carlsbad, CA), following the manufacturer's instructions. Bacterial 16S rRNA amplicons of the V3-V4 regions of bacterial communities were obtained using the primers 341F (5'-CCTAYGGGRBGCASCAG-3') and 806R (5'-GGACTACHVGGGTWTCTAAT-3') (Caporaso et al., 2012). PCR amplicons were pooled at equimolar concentrations and were submitted for commercial

paired-end sequencing on an Illumina MiSeq. PCR amplification and Illumina Miseq sequencing were performed by Shanghai Biozeron Bio-Pharm Technology Co., Ltd. (Shanghai, China). Through quality checking, barcodes and primers of raw illumina paired-end reads that exceeded 75% of the amplicon length were trimmed off and combined using Flash v1.2.7. Data for all samples are available on the Sequence Read Archive (http://www.ncbi.nlm.nih.gov/sra/) project reference SRP212348.

2.5 Sequence analyses and functional gene prediction

Sequence analysis was performed using QIIME v1.9.0 (Caporaso et al., 2010). 29355 operational taxonomic units (OTUs) were assigned using Uclust (Edgar 2010) based on 97% identity. A representative sequence from each OTU was classified using the Ribosomal Database Project (RDP) classifier (Wang et al., 2007) and a training set extracted from the Silva v128 reference database.

The functional potentials of bacterial communities under different conditions were predicted using PICRUSt 1.1.0 (Langille et al., 2013). Based on the 16S rRNA sequences and the genome database, PICRUSt was employed to predict the functional composition of a metagenome. Clustered OTUs were used to pick the sampled reads against the Greengenes 13.5 database. The 16S rRNA gene copy number was normalized using a normalized OTU table. Finally, the metagenome prediction of molecular functions was categorized into Kyoto Encyclopedia of Genes and Genomes (KEGG) Orthologs (KOs) at 1–3 pathway levels.

2.6 Statistical analyses

To investigate whether the relative abundance of the microbial community was significantly different between treatments, a one-way analysis of variance (ANOVA) was conducted. Relationships between bacterial assemblages were calculated by non-metric multidimensional scaling (NMDS; Bray–Curtis distance) ordination. Analysis of similarities (ANOSIM) based on NMDS was used to investigate significant differences among microbial communities.

To investigate whether taxonomic and relative abundances of functional gene categories were significantly different under various DOM backgrounds, Lefse and Statistical Analysis of Metagenomic Profiles (STAMP) analyses were conducted. The software STAMP v.2.1.3 was used to analyze the KEGG abundance profile to identify significant pathways for metabolism between groups using a two sided Welch's t-test. Heatmaps were created to investigate metabolic functional differences between communities based on the Bray–Curtis distance.

Understanding the interactions between the microbial community and DOM is essential to identify community assembly rules for utilizing the organic matrix. The co-occurrence of bacterial OTUs and fluorescent intensities of PARAFAC components was identified via MINE statistics by calculating the maximal information coefficient (MIC) (Reshef et al., 2011). MIC analysis can capture a wide range of correlations between data pairs, which contain both linearity and nonlinearity. Multiple testing corrections accounted for the use of the false discovery rate (FDR) to modulate P-values (Benjamini and Hochberg 1995). False discovery rates were

calculated using the R package locfdr (Efron 2004). The correlation was considered significant when FDR was < 1%, which was equivalent to MIC > 0.497. The matrix of MIC values > 0.497 was used with Gephi v.9.1 to visualize the network of corresponding to positive linear correlations. In these visualizations, bacterial OTUs and DOM components are represented as nodes that are connected by lines, proportional in length to the MIC value. Pearson product moment correlations were used to determine significant relationships (P values < 0.05) between metabolic function and significantly variable bacteria of phylogenetic structure among groups. These correlations were conducted using R and were visualized using a heatmap in which P-values were opposed to an α-value of 0.05.

3. Results and discussion

3.1 Change of DOM in fluorescence

DOC concentrations varied among confluent sites *in situ* (Supplementary Table S1). These ranged from 9.55 to 16.3 mg/L following the sequence of SCE > JXZ > DWS > QHR. Previous research pointed out that DOC are transported through estuaries to oceans (Seitzinger and Sanders 1997), which could explain that DOC were more abundant in estuary areas than in inland rivers.

PARAFAC analysis identified six distinct fluorescent components for EEM at all samples (Table 1), describing 98.83% of the variability within data. The PARAFAC model was compared against other published models in the Openfluor database, where ⩾ 93.8% similarity matched to models. Component one (C1) depicted

characteristics as microbially DOM with fewer aromatic structures (Peleato et al., 2017). Component two (C2), categorized as the previously defined humic-and-fulvic-like material, was common in aquatic environment (e.g. stream, river, estuary, lakes, wetlands, and shelf seas) (Lapierre and del Giorgio 2014). Component three (C3) was previously reported to be related to proteinaceous tryptophan-like matter (Cohen et al., 2014).

Component four (C4) showed locations of maximum peak intensities that are typical for what has been referred to as a combination of marine humic-like peak M and terrestrially humic peak A (Shutova et al., 2014). Both C3 and C4 can be found in wastewater; however, C4 could either originate from recycled water, greywater stream or treated drinking water (Murphy et al., 2011). The JXZ sample, originated from WWTP, contained higher abundances of proteins and humic substances (Figure 1), similar as the results reported by previous study (Yang et al., 2014). Component five (C5) possessed low Ex-EM wavelength fluorescence and was identified as a combination of protein-like and tannin-like (D'Andrilli et al., 2017). Based on lower molecular weights and aromaticity, C5 was confirmed to have higher bio-availability (Cohen et al., 2014). Confluence area like DWS and QHR had more abundant C5 constituent. Component six (C6) exhibited fluorescence properties similar to humic- and tryptophan-like DOM (Jorgensen et al., 2011), which was abundant in SCE and QHR samples.

The spectra and fluorescence intensities of six DOM components changed in four experimental treatments were shown in Figure 1. During the initial 12 h after

inoculation, the fluorescence intensities of most humic-like DOM and few proteinaceous DOM decreased, which was also found in previous research (Young et al., 2004). This suggests that the loss of humus within a short incubation period could be explained as bacterial metabolism and the adsorption of humic matter onto bacterial cell walls along with other dissolved solids or inorganic colloids (Docherty et al., 2006). Compared with other confluence area, most components, including protein-like and humic-like matter, turned more active in SCE and WWTP area. C4 showed similar fluctuation trends in all samples. C5 exhibited strong changes, suggesting that it was more labile than other organics. As major component of tannins and humic DOM, compositions like C5 commonly exists in the aquatic system and were similar to fluorophore peak B (tyrosine-like; Ex: 240; Em: 300 nm). Moreover, the mineralization and remineralization processes caused a change of organic compounds in quantity. It was confirmed that the utilization of the same DOM component could vary over different water backgrounds. However, humus was less disturbed by various confluent environments. Finally, the humification degree decreased in SCE and JXZ and increased in both QHR and DWS. Therefore, these results suggest that amino-like DOM can be rapidly utilized in all areas, and the humification process will be accelerated in the confluence zone with high percentages of humic-like DOM.

3.2 Shifts in Bacterial Community Composition

In response to DOM loads, the individual populations (i.e., OTUs) were

examined, which contributed significantly to the differences in community composition between treatments from the start to the end of the experiment. Following quality filtering, a total of 29,355 reads were obtained from 41 samples (36 experimental samples and 5 control samples). Experimental samples contained an average of 6583 OTUs. Bacterial communities under the four treatments were distinct from one another in composition and varied at the temporal scale (Figure 2). Almost all reads were mainly assignable to eight phyla. The results implied that in all microbial communities, the four dominant phyla were Proteobacteria, Bacteroidetes, and Actinobacteria. Proteobacteria have been reported to be able to decompose soluble sugars into both monosaccharides and short chain fatty acids (Xu et al., 2017). It has been reported that Proteobacteria could be strongly influenced by lipid and humic-like DOM, while Actinobacteria were reported to be significantly adjusted by aromatic and humic-like DOM (Liu et al., 2019). Bacteroidetes, which are common and widespread in surface water bacterial communities, were functional in decomposing hydrolytic cellulose, starch polysaccharides, and carbohydrate (Reddy et al., 2019) and have been reported to respond rapidly and remineralize complex and labile DOM (Bauer et al., 2006). Similar research, which focused on the effect of DOM addition to bacterial community, reported that Bacteroidetes, Alpha-, and Betaproteobacteria were the particularly dominant phylum in response to elevated DOM levels (Traving et al., 2017).

Significant differences were found among samples in the relative abundance of Deltaproteobacteria ($P < 0.05$). Taxonomic differences among different treatment over

time were evident. Both Betaproteobacteria and Actinobacteria followed a trend of fluctuating decline in all conditions, and a particular proliferation of Betaproteobacteria occurred in the JXZ treatment. In contrast, the relative abundance of Alphaproteobacteria increased with fluctuation, and Bacteroidetes increased at the beginning, which was followed by a decrease. The abundance of Deltaproteobacteria shifted between the control and other DOM liquor. Bacterial communities were significantly clustered according to the treatment (Figure 3, $P = 0.01$). Moreover, the communities in the same sampling time among groups were taxonomically similar. Cyanobacteria and Verrucomicbia were closer to each other (low Bray–Curtis distance, Figure 3) than other genera.

Experimental bacterial assemblages with DOM addition differed in composition compared to control samples, and the distances subsequently shortened in non-metric multidimensional scaling ordination (Figure 4). ANOSIM analysis also showed a significant distinction ($P < 0.05$) in five DOM backgrounds including control. There were no significant differences ($P = 0.107$) in four treatment except for the control sample. This indicates that DOM play a significant role in the shaping of the structure of the microbial community and impact its composition.

3.3 Comparison of functional properties between different treatment

Functional differences among different treatments were clearly found in a comparison of the relative abundance of the PICRUSt predicted KEGG orthologies (KOs) classified at level-2-involved metabolic pathways (Figure S1). Pathways that

are indicative of metabolic functions were clearly higher in the DWS treatment, which may be due to the similarity of DWS and inoculated primary environment. These major gene categories were significantly different in abundance among microbial communities in different DOM treatment ($P < 0.05$, Figure 5). The activities of lipid metabolism (ether lipid metabolism) followed the sequence of JXZ > SCE > DWS > QHR. Similarly, it was found that addition of high molecular weight DOM from surface seawater to microbial communities enriched genes that are involved in the lipid metabolism (McCarren et al., 2010). Therefore, the result indicates that the more humic-like DOM converge, the more active lipid metabolisms will be induced at the confluence. With regard to the metabolism of cofactors and vitamins (one carbon pool by folate) and amino acid metabolism (lysine degradation), the sequences followed: QHR > DWS > SCE and DWS > SCE > QHR. Both metabolic pathways were strongly associated with the degradation of alanine, aspartate, glutamate, and other carbohydrates (Neis et al., 2015). The pathways of the energy metabolism (carbon fixation pathways in prokaryotes) were significantly higher in QHR and JXZ, compared with that in SCE and DWS ($P < 0.05$). This indicates an acceleration of nutrient conversion and a depletion of the available organic carbon (Shi et al., 2017) in QHR and JXZ.

Microbial functional genes, related to the lipid metabolism (arachidonic acid metabolism) were significantly more expressed in SCE, compared with that in QHR, DWS, and JXZ ($P < 0.05$). Furthermore, genes related to the carbohydrate metabolism (propanoate metabolism and galactose metabolism), were higher in SCE than those at

DWS and JXZ ($P < 0.05$). This suggested that the rates of carbon turnover and utilization capacity of carbon sources by bacterial community were higher (Zhou et al., 2019) in SCE. However, functional genes that are linked to the carbohydrate metabolism (glycolysis/gluconeogenesis and inositol phosphate metabolism), and xenobiotics biodegradation and metabolism (fluorobenzoate degradation) were significantly lower in JXZ ($P < 0.05$). This may be related to the high percentage of humic components.

Compared with SCE, QHR, and JXZ, the functional genes that are involved in the amino acid metabolism (phenylalanine, tyrosine, and tryptophan biosynthesis), metabolism of cofactors and vitamins (retinol metabolism), and biosynthesis of other secondary metabolites (isoquinoline alkaloid biosynthesis) were significantly lower in DWS ($P < 0.05$). This implies that the biodegradations of labile substances (e.g. amino acids) were less active in DWS. Additionally, functional genes linked with the metabolism of terpenoids and polyketides (geraniol degradation) and xenobiotics biodegradation and metabolism (caprolactam degradation) were higher in DWS than in SCE and QHR ($P < 0.05$). Similar results were reported, which indicates that refractory organics could be mainly degraded by thermophilic bacteria (Wang et al., 2018). All of the above may contribute to higher abundances of metabolic function (level-2) in DWS than in other DOM backgrounds.

3.4 Co-occurrence between community composition and DOM components, metabolic function and DOM components

MIC analysis provided information about direct associations between FI and relative abundances of the most abundant bacterial taxa at the end of the experiment (classified predominantly as Proteobacteria and, to a far lesser extent, Bacteroidetes; as shown in Figure 6). It was found that 199, 217, 25 and119 OTUs had associations with various DOM components in SCE, QHR, DWS and JXZ samples respectively. Actinobacteria, Bacteroidetes, and Proteobacteria were highly relevant to DOM components. Different taxa involved in metabolizing DOM components with various characteristics. Alphaproteobacteria (OTU 3912), Gammaproteobacteria (OTU 2010), and Verrucomicrobia (OTU 2902), showed positive correlations with C2 both in SCE and QHR, implying that these OTUs were close to humic-like DOM. Actinobacteria (OTU 296), Betaproteobacteria (OTU 4965), Gammaproteobacteria (OTU 163, 1047, 1769, and 3456), Deltaproteobacteria (OTU 162), and Verrucomicrobia (OTU 82) had close links with protein-like and amino acids-like components. Gemmatimonadetes and Planctomycetes had close connections with humic-like and amino acids-like components in SCE and JXZ area. Both phyla exist in aquatic and terrestrial ecosystems (Ward et al., 2006), and members of Gemmatimonadetes were reported to be highly abundant after DOM addition (Traving et al., 2017). As minor phyla in freshwater, populations of Verrucomicrobia and Planctomycetes were suggested to participate in *N*-acetyl-glucosamine (NAG) degradation in lakes (Tada and Grossart 2014). Compared with other DOM components, humic-like components C2, C4, and

C6 exhibited a higher degree of connectivity with OTU. C1, C2 and C4 formed closely related groups in JXZ. Moreover, the highly active component C5 was bound to Proteobacteria, Verrucomicrobia, and Actinobacteria in SCE, QHR, and DWS. Proteobacteria have been confirmed to be significantly linked to DOM concentration and/or composition (Amaral et al., 2016). Actinobacteria are abundant in freshwaters and involved in DOM hydrolysis process (Kirchman et al., 2004; Ma et al., 2019). Deltaproteobacteria were found to be strongly correlated with C5 and C6 (SCE), C1, C3, C4, and C5 (QHR), and C6 (JXZ), suggesting that both humic-like and protein-like DOM may be contributing factors to the significant difference of this class among groups.

Most protein-like and humic-like organic matter exhibited high associations with OTU in the MIC analysis. A number of studies indicated that the distribution and dynamic changes of the humic substances follow pronounced correlations with the production of microbial metabolites (Lee et al., 2019), even though humic-like DOM coagulated through abiotic self-assembly are more resistant to microbial utilization compared to both carbohydrates and protein-like DOM (Beier et al., 2015). Compared to low molecular weight DOM, the high molecular weight organics were generally characterized with high hydrophobic properties and numerous functional groups (Xu et al., 2019). A previous study showed that bacteria were able to consume refractory DOM, the microbial reworking of, which is important in freshwater systems (Docherty et al., 2006). It can be inferred that humic-like matter together with most protein or tyrosine like substances is closely linked to microbes, which may be due to

the unique and functional compositions and impact ecosystem function.

To better understand the relationship between DOM and the microbial community for the utilization and degradation process, further research was conducted on the functional level. Through Lefse analysis, various genera among groups have been selected (Figure S2). Pearson product moment correlations were calculated to explore significant relationships (P values < 0.01, Rho values > 0.9) between metabolic function and bacteria indicative of group difference (Figure S3). Energy metabolism (carbon fixation pathways in prokaryotes) and xenobiotics biodegradation and metabolism (caprolactam degradation) were significantly associated with Proteobacteria (*Sphingomonas* and *Acinetobacter*) in all treatments and highly correlated in QHR and DWS. The active carbon fixation function and genera that were significantly linked with this function may explain the observed increase of fluorescence intensity during the cultivation process. This suggests that the microbial utilization of DOM in DWS may be due to the function of caprolactam degradation. The lipid metabolism (arachidonic acid metabolism) was only highly correlated with Proteobacteria (*Sphingopyxis*) in SCE, which corresponds to the result of the functional prediction and might be linked to a shift of amino acid like matter such as C2 in SCE. However, the metabolism of cofactors and vitamins (retinol metabolism) was also closely linked to Proteobacteria (*Candidatus Accumulibacter*) only in DWS, which did not match the functional prediction.

By comparing the results of MIC and Pearson analysis, Sphingomonas varied among groups and were found to be significantly correlated to both DOM components

and metabolism function. The variation of the microbial community in composition or function between treatments may be due to utilizing DOM (containing humic-like, protein-like, and tannin-like DOM) through this genus. Furthermore, not every component in different confluence area had the same degrading tendency and correlation with microbes, e.g., C1 in QHR and JXZ samples, and C3 in SCE and QHR samples. The degree of DOM biodegradation depends on not only the microbial community structure but also the chemical properties of DOM components. Moreover, the observed fluorescent dissolved organic matter (fDOM) are a subset of the total DOM pool (Stubbins et al., 2014), which suggested that the remaining DOM may also contribute to the degrading processes. Meanwhile, various bacterial phylogenetic communities are dominant in different compositions of DOM (Cottrell and Kirchman 2000), and responses of a number of bacteria to various amino acid were completely different in that they were auxotrophic for specific amino acids (Tripp et al., 2009). DOM is an assemblage of many components, and the biodegradation of one ingredient may change according to the characteristics of other composed organic matter. These results suggested that the source, quality, and quantity of DOM varied in different river confluences, and a number of DOM components overlapped, which would induce a change of microbial phylogeny and exert significant impacts on the metabolic balance of pools or river systems.

4. Conclusions

In the natural inland watershed, the influence zone, composed by the accepted

river and its input rivers, is highly complex. Various DOM originating from different flows and background interact with each other and impact both the microbial community and the ecosystem. This study documented the changes of different converged DOM, biodegraded by the same bacterial community and detailed the response of community in taxonomy and metabolic function. Significant shifts of taxa at the genus level structure and level-2 metabolic function were found among groups. EEM-PARAFAC analysis indicated that most DOM components shifted differently in various conditions. Moreover, even though organics like protein and amino acid were first utilized, humics showed more abundant correlation with community and microbial metabolism.

Actinobacteria, Proteobacteria, Bacteroidetes, and Verrucomicrobia were found to be closely linked to the degradation of humic-like matter. Moreover, the results of OTU filtering correlated with DOM and genera associated with metabolic function overlapped (Proteobacteria (*Sphingomonas*)). This suggests that the coinciding microbes may be the key for the exploration of the biodegradation process of DOM. Deltaproteobacteria turned to be significantly different even though the whole bacterial phylogeny were not significantly different among various DOM background. The metabolism of the same microbial community shaped differently when facing DOM in various urban river confluences. The utilization capacity of carbon sources by the bacterial community were higher in the estuary. The metabolic function was more abundant at the intersection of source water and urban rivers. The abundance of the microbial metabolism was lower downstream of the WWTP effluent. This work

offers a method to investigate the biodegraded of various DOM compounds and provides a basis for the exploration of the interaction of DOM and the microbial community at different river confluence reaches.

Acknowledgements

The study was financially supported by the National Natural Science Foundation of China (51779076, 51879079), the Fundamental Research Funds for the Central Universities (2019B52514), the Foundation for Innovative Research Groups of the National Natural Science Foundation of China (51421006), the Priority Academic Program Development of Jiangsu Higher Education Institutions, and the Top-Notch Academic Programs Project of Jiangsu Higher Education Institutions (TAPP).

Supplementary information

One table and three figures are provided in the Supporting Information sections to present detailed informations. The first section is the supplementary table which shows physiochemical characteristics of four investigated confluence samples. The second section is the supplementary figures, which presents the relative abundance of predicted functions and selected indicative species in different groups. The third section is the supplementary figure, which shows correlations between various indicator genera and functions (level-3 metabolism).

488 # References

489 Amaral, V., Graeber, D., Calliari, D. and Alonso, C. (2016) Strong linkages between
490 DOM optical properties and main clades of aquatic bacteria. Limnology and
491 Oceanography 61(3), 906-918.

492 Bauer, M., Kube, M., Teeling, H., Richter, M., Lombardot, T. and Allers, E. (2006)
493 Whole genome analysis of the marine Bacteroidetes 'Gramella forsetii' reveals
494 adaptations to degradation of polymeric organic matter. Environmental
495 Microbiology 8(12), 2201-2213.

496 Beier, S., Rivers, A.R., Moran, M.A. and Obernosterer, I. (2015) The transcriptional
497 response of prokaryotes to phytoplankton-derived dissolved organic matter in
498 seawater. Environmental Microbiology 17(10), 3466-3480.

499 Benda, L., Poff, N.L., Miller, D., Dunne, T., Reeves, G., Pess, G. and Pollock, M.
500 (2004) The network dynamics hypothesis: How channel networks structure
501 riverine habitats. Bioscience 54(5), 413-427.

502 Benjamini, Y. and Hochberg, Y. (1995) Controlling the False Discovery Rate: a
503 Practical and Powerful Approach to Multiple Testing. Journal of the Royal
504 Statistical Society 57(1), 289-300.

505 Caporaso, J.G., Kuczynski, J., Stombaugh, J., Bittinger, K., Bushman, F.D., Costello,
506 E.K., Fierer, N., Pena, A.G., Goodrich, J.K., Gordon, J.I., Huttley, G.A., Kelley,
507 S.T., Knights, D., Koenig, J.E., Ley, R.E., Lozupone, C.A., McDonald, D.,
508 Muegge, B.D., Pirrung, M., Reeder, J., Sevinsky, J.R., Tumbaugh, P.J., Walters,
509 W.A., Widmann, J., Yatsunenko, T., Zaneveld, J. and Knight, R. (2010) QIIME

allows analysis of high-throughput community sequencing data. Nature Methods 7(5), 335-336.

Caporaso, J.G., Lauber, C.L., Walters, W.A., Berg-Lyons, D., Huntley, J., Fierer, N., Owens, S.M., Betley, J., Fraser, L., Bauer, M., Gormley, N., Gilbert, J.A., Smith, G. and Knight, R. (2012) Ultra-high-throughput microbial community analysis on the Illumina HiSeq and MiSeq platforms. The ISME Journal 6(8), 1621-1624.

Cohen, E., Levy, G.J. and Borisover, M. (2014) Fluorescent components of organic matter in wastewater: efficacy and selectivity of the water treatment. Water Research 55, 323-334.

Cottrell, M.T. and Kirchman, D.L. (2000) Natural assemblages of marine proteobacteria and members of the Cytophaga-Flavobacter cluster consuming low- and high-molecularweight dissolved organic matter. Applied Environment Microbiology 66(4), 1692-1697.

D'Andrilli, J., Foreman, C.M., Sigl, M., Priscu, J.C. and McConnell, J.R. (2017) A 21 000-year record of fluorescent organic matter markers in the WAIS Divide ice core. Climate of the Past 13(5), 533-544.

Docherty, K.M., Young, K.C., Maurice, P.A. and Bridgham, S.D. (2006) Dissolved organic matter concentration and quality influences upon structure and function of freshwater microbial communities. Microbial Ecology 52(3), 378-388.

Du, Y., Zhang, Q., Liu, Z., He, H., Lurling, M., Chen, M. and Zhang, Y. (2019) Composition of dissolved organic matter controls interactions with La and Al

ions: Implications for phosphorus immobilization in eutrophic lakes. Environmental Pollution 248, 36-47.

Edgar, R.C. (2010) Search and clustering orders of magnitude faster than BLAST. Bioinformatics 26(19), 2460-2461.

Efron, B. (2004) Large-scale simultaneous hypothesis testing: The choice of a null hypothesis. Journal of the American Statistical Association 99(465), 96-104.

Grinsted, A., Moore, J.C. and Jevrejeva, S. (2013) Projected Atlantic hurricane surge threat from rising temperatures. Proceedings of the National Academy of Sciences of the United States of America 110(14), 5369-5373.

Gualtieri, C., Ianniruberto, M., Filizola, N., Santos, R. and Endreny, T. (2017) Hydraulic complexity at a large river confluence in the Amazon basin. Ecohydrology 10(7), 12.

Guenther, M. and Valentin, J.L. (2009) Bacterial and phytoplankton production in two coastal systems influenced by distinct eutrophication processes. Oecologia Brasiliensis (12), 172-178.

Guo, W., Yang, L., Zhai, W., Chen, W., Osburn, C.L., Huang, X. and Li, Y. (2014) Runoff-mediated seasonal oscillation in the dynamics of dissolved organic matter in different branches of a large bifurcated estuaryThe Changjiang Estuary. Journal of Geophysical Research-Biogeosciences 119(5), 776-793.

Hijnen, W.A.M., Beerendonk, E.F. and Medema, G.J. (2006) Inactivation credit of UV radiation for viruses, bacteria and protozoan (oo)cysts in water: A review. Water Research 40(1), 3-22.

553 Holland, A., Stauber, J., Wood, C.M., Trenfield, M. and Jolley, D.F. (2018) Dissolved
554 organic matter signatures vary between naturally acidic, circumneutral and
555 groundwater-fed freshwaters in Australia. Water Research 137, 184-192.
556 Jansson, M., Persson, L., De Roos, A.M., Jones, R.I. and Tranvik, L.J. (2007)
557 Terrestrial carbon and intraspecific size-variation shape lake ecosystems. Trends
558 in Ecology & Evolution 22(6), 316-322.
559 Jorgensen, L., Stedmon, C.A., Kragh, T., Markager, S., Middelboe, M. and
560 Sondergaard, M. (2011) Global trends in the fluorescence characteristics and
561 distribution of marine dissolved organic matter. Marine Chemistry 126(1-4),
562 139-148.
563 Kaartokallio, H., Asmala, E., Autio, R. and Thomas, D.N. (2016) Bacterial production,
564 abundance and cell properties in boreal estuaries: relation to dissolved organic
565 matter quantity and quality. Aquatic Sciences 78(3), 525-540.
566 Kirchman, D.L., Dittel, A.I., Findlay, S.E.G. and Fischer, D. (2004) Changes in
567 bacterial activity and community structure in response to dissolved organic
568 matter in the Hudson River, New York. Aquatic Microbial Ecology 35(3),
569 243-257.
570 Lakowicz, J.R. (2013) Principles of fluorescence spectroscopy, Springer Science &
571 Business Media.
572 Landa, M., Cottrell, M.T., Kirchman, D.L., Kaiser, K., Medeiros, P.M., Tremblay, L.,
573 Batailler, N., Caparros, J., Catala, P., Escoubeyrou, K., Oriol, L., Blain, S. and
574 Obernosterer, I. (2014) Phylogenetic and structural response of heterotrophic

bacteria to dissolved organic matter of different chemical composition in a continuous culture study. Environmental Microbiology 16(6), 1668-1681.

Langille, M.G.I., Zaneveld, J., Caporaso, J.G., McDonald, D., Knights, D., Reyes, J.A., Clemente, J.C., Burkepile, D.E., Thurber, R.L.V., Knight, R., Beiko, R.G. and Huttenhower, C. (2013) Predictive functional profiling of microbial communities using 16S rRNA marker gene sequences. Nature Biotechnology 31(9), 814-836.

Lapierre, J.F. and del Giorgio, P.A. (2014) Partial coupling and differential regulation of biologically and photochemically labile dissolved organic carbon across boreal aquatic networks. Biogeosciences 11(20), 5969-5985.

Lee, Y.K., Lee, M.H. and Hur, J. (2019) A new molecular weight (MW) descriptor of dissolved organic matter to represent the MW-dependent distribution of aromatic condensation: Insights from biodegradation and pyrene binding experiments. Science of the Total Environment 660, 169-176.

Liu, S.J., Xi, B.D., Qiu, Z.P., He, X.S., Zhang, H., Dang, Q.L., Zhao, X.Y. and Li, D. (2019) Succession and diversity of microbial communities in landfills with depths and ages and its association with dissolved organic matter and heavy metals. Science of the Total Environment 651, 909-916.

Logue, J.B., Stedmon, C.A., Kellerman, A.M., Nielsen, N.J., Andersson, A.F., Laudon, H., Lindstrom, E.S. and Kritzberg, E.S. (2016) Experimental insights into the importance of aquatic bacterial community composition to the degradation of dissolved organic matter. The ISME Journal 10(3), 533-545.

Ma, S.J., Ma, H.J., Hu, H.D. and Ren, H.Q. (2019) Effect of mixing intensity on hydrolysis and acidification of sewage sludge in two-stage anaerobic digestion: Characteristics of dissolved organic matter and the key microorganisms. Water Research 148, 359-367.

McCarren, J., Becker, J.W., Repeta, D.J., Shi, Y., Young, C.R., Malmstrom, R.R., Chisholm, S.W. and DeLong, E.F. (2010) Microbial community transcriptomes reveal microbes and metabolic pathways associated with dissolved organic matter turnover in the sea. Proceedings of the National Academy of Sciences of the United States of America 107(38), 16420-16427.

Murphy, K.R., Hambly, A., Singh, S., Henderson, R.K., Baker, A., Stuetz, R. and Khan, S.J. (2011) Organic Matter Fluorescence in Municipal Water Recycling Schemes: Toward a Unified PARAFAC Model. Environmental Science & Technology 45(7), 2909-2916.

Neis, E.P.J.G., Dejong, C.H.C. and Rensen, S.S. (2015) The Role of Microbial Amino Acid Metabolism in Host Metabolism. Nutrients 7(4), 2930-2946.

Peleato, N.M., Sidhu, B.S., Legge, R.L. and Andrews, R.C. (2017) Investigation of ozone and peroxone impacts on natural organic matter character and biofiltration performance using fluorescence spectroscopy. Chemosphere 172, 225-233.

Reddy, B., Pandey, J. and Dubey, S.K. (2019) Assessment of environmental gene tags linked with carbohydrate metabolism and chemolithotrophy associated microbial community in River Ganga. Gene 704, 31-41.

618 Reshef, D.N., Reshef, Y.A., Finucane, H.K., Grossman, S.R., McVean, G., Turnbaugh,
619 P.J., Lander, E.S., Mitzenmacher, M. and Sabeti, P.C. (2011) Detecting Novel
620 Associations in Large Data Sets. Science 334(6062), 1518-1524.
621 Rice, S.P. (2017) Tributary connectivity, confluence aggradation and network
622 biodiversity. Geomorphology 277, 6-16.
623 Richards, K.S. (1980) A note on changes in channel geometry at tributary junctions.
624 Water Resources Research 16(1), 241-244.
625 Saarenheimo, J., Aalto, S.L., Rissanen, A.J. and Tiirola, M. (2017) Microbial
626 Community Response on Wastewater Discharge in Boreal Lake Sediments.
627 Frontiers in Microbiology 8, 1-12.
628 Seitzinger, S.P. and Sanders, R.W. (1997) Contribution of dissolved organic nitrogen
629 from rivers to estuarine eutrophication. Marine Ecology Progress Series 159,
630 1-12.
631 Shi, L., Huang, Y., Zhang, M., Yu, Y., Lu, Y. and Kong, F. (2017) Bacterial
632 community dynamics and functional variation during the long-term
633 decomposition of cyanobacterial blooms in-vitro. Science of the Total
634 Environment 598, 77-86.
635 Shutova, Y., Baker, A., Bridgeman, J. and Henderson, R.K. (2014) Spectroscopic
636 characterisation of dissolved organic matter changes in drinking water treatment:
637 From PARAFAC analysis to online monitoring wavelengths. Water Research 54,
638 159-169.

639 Stedmon, C.A. and Bro, R. (2008) Characterizing dissolved organic matter
640 fluorescence with parallel factor analysis: a tutorial. Limnology and
641 Oceanography Methods 6(11), 572-579.
642 Stedmon, C.A., Thomas, D.N., Papadimitriou, S., Granskog, M.A. and Dieckmann,
643 G.S. (2011) Using fluorescence to characterize dissolved organic matter in
644 Antarctic sea ice brines. Journal of Geophysical Research Biogeosciences 116,
645 1-9.
646 Stubbins, A., Lapierre, J.F., Berggren, M., Prairie, Y.T., Dittmar, T. and del Giorgio,
647 P.A. (2014) What's in an EEM? Molecular signatures associated with dissolved
648 organic fluorescence in boreal Canada. Environmental Science & Technology
649 48(18), 10598-10606.
650 Tada, Y. and Grossart, H.P. (2014) Community shifts of actively growing lake bacteria
651 after N-acetyl-glucosamine addition: improving the BrdU-FACS method. The
652 ISME Journal 8(2), 441-454.
653 Traving, S.J., Rowe, O., Jakobsen, N.M., Sorensen, H., Dinasquet, J., Stedmon, C.A.,
654 Andersson, A. and Riemann, L. (2017) The Effect of Increased Loads of
655 Dissolved Organic Matter on Estuarine Microbial Community Composition and
656 Function. Frontiers in Microbiology 8, 1-15.
657 Tripp, H.J., Schwalbach, M.S., Meyer, M.M., Kitner, J.B., Breaker, R.R. and
658 Giovannoni, S.J. (2009) Unique glycine-activated riboswitch linked to
659 glycine-serine auxotrophy in SAR11. Environmental Microbiology 11(1),
660 230-238.

661 Wang, K., Mao, H. and Li, X. (2018) Functional characteristics and influence factors
662 of microbial community in sewage sludge composting with inorganic bulking
663 agent. Bioresource Technology 249, 527-535.
664 Wang, Q., Garrity, G.M., Tiedje, J.M. and Cole, J.R. (2007) Naive Bayesian classifier
665 for rapid assignment of rRNA sequences into the new bacterial taxonomy.
666 Applied and Environmental Microbiology 73(16), 5261-5267.
667 Ward, N., Staley, J.T., Fuerst, J.A., Giovannoni, S., Schlesner, H. and and
668 Stackebrandt, E. (2006) The Order Planctomycetales, Including the Genera
669 Planctomyces, Pirellula, Gemmata and Isosphaera and the Candidatus Genera
670 Brocadia, Kuenenia and Scalindua. Berlin: Springer.
671 Xu, H., Ji, L., Kong, M., Jiang, H. and Chen, J. (2019) Molecular weight-dependent
672 adsorption fractionation of natural organic matter on ferrihydrite colloids in
673 aquatic environment. Chemical Engineering Journal 363, 356-364.
674 Xu, H.C., Houghton, E.M., Houghton, C.J. and Guo, L.D. (2018) Variations in size
675 and composition of colloidal organic matter in a negative freshwater estuary.
676 Science of the Total Environment 615, 931-941.
677 Xu, S., Lu, W., Liu, Y., Ming, Z., Liu, Y., Meng, R. and Wang, H. (2017) Structure
678 and diversity of bacterial communities in two large sanitary landfills in China as
679 revealed by high-throughput sequencing (MiSeq). Waste Management 63, 41-48.
680 Yang, X.F., Meng, F.G., Huang, G.C., Sun, L. and Lin, Z. (2014) Sunlight-induced
681 changes in chromophores and fluorophores of wastewater-derived organic matter
682 in receiving waters - The role of salinity. Water Research 62, 281-292.

683 Young, K.C., Maurice, P.A., Docherty, K.M. and Bridgham, S.D. (2004) Bacterial
684 Degradation of Dissolved Organic Matter from Two Northern Michigan Streams.
685 Geomicrobiology Journal 21(8), 521-528.
686 Zepp, R.G., Sheldon, W.M. and Moran, M.A. (2004) Dissolved organic fluorophores
687 in southeastern US coastal waters: correction method for eliminating Rayleigh
688 and Raman scattering peaks in excitation-emission matrices. Marine Chemistry
689 89(1-4), 15-36.
690 Zhou, G., Qiu, X., Chen, L., Zhang, C., Ma, D. and Zhang, J. (2019) Succession of
691 organics metabolic function of bacterial community in response to addition of
692 earthworm casts and zeolite in maize straw composting. Bioresource Technology
693 280, 229-238.
694 Zhou, L., Zhou, Y., Hu, Y., Cai, J., Bai, C., Shao, K., Gao, G., Zhang, Y., Jeppesen, E.
695 and Tang, X. (2017) Hydraulic connectivity and evaporation control the water
696 quality and sources of chromophoric dissolved organic matter in Lake Bosten in
697 arid northwest China. Chemosphere 188, 608-617.
698 Zhou, Y.Q., Zhang, Y.L., Jeppesen, E., Murphy, K.R., Shi, K., Liu, M.L., Liu, X.H.
699 and Zhu, G.W. (2016) Inflow rate-driven changes in the composition and
700 dynamics of chromophoric dissolved organic matter in a large drinking water
701 lake. Water Research 100, 211-221.
702

Tables

Table 1 The PARAFAC component matches with other freshwater components in the Openfluor database and their associated details.

Figure captions

Figure 1 Spectra of the six main components determined via PARAFAC analysis (a) and fluorescent intensities of components (b). (a) EEMs collected from the beginning to the end of experiment across the three replicates for each treatment (n = 3). (b) Insets visualise the respective spectral properties of the six fluorescent components identified by PARAFAC analysis.

Figure 2 Taxonomic composition of bacterial experimental communities as relative abundances of each phylum. Proteobacteria and Actinobacteria are identified to class level. 1-1 to 1-9 represent the samples of SCE, 2-1 to 2-9 represent the samples of QHR, 3-1 to 3-9 represent the samples of DWS, 4-1 to 4-9 represent the samples of JXZ, and 5-1 to 5-9 represent the samples of Control.

Figure 3 Heatmap showing the taxonomic differences of microbial communities in different treatments based on the Bray–Curtis distance. Bray–Curtis distances were calculated using relative abundances of OTUs.

Figure 4 NMDS representation of bacterial community in five experimental environments. NMDS ordination was derived from pairwise Bray–Curtis distances. S1-S9 represent the microbial community of SCE, Q1-Q9 represent the microbial community of QHR, D1-D9 represent the microbial community of DWS, J1-J9 represent the microbial community of JXZ, and C1-C9 represent the microbial community of Control.

Figure 5 The functional composition of significant changes in intestinal bacterial Kyoto Encyclopedia of Genes and Genomes (KEGG) pathways of level-3 metabolic categories between SCE and QHR, SCE and DWS, SCE and JXZ, QHR and DWS, QHR and JXZ, or DWS and JXZ using the response ratio method at a 95% confidence interval (CI).

Figure 6. Associations between DOM components (triangles) and bacterial OTUs (circles) in (a) SCE, (b) QHR, (c) DWS, and (d) JXZ, identified with MIC statistics and visualized as a network. C1-C6 were the DOM components identified by EEM-PARAFAC analysis. The sizes of the circles are proportional to the relative abundance of the OTU.

742 Table 1 The PARAFAC component matches with other freshwater components in the
743 Openfluor database and their associated details.

Component	Ex (max)/ nm	Em (max)/ nm	TCC*	Details	Reference
C1	310	385	0.987	Microbially DOM with fewer aromatic structures	Peleato et al. 2016
C2	275	430	0.938	Humic- and fulvic-like material	Lapierre et al. 2014
C3	275	330	0.981	Proteinaceous tryptophan-like matter	Cohen et al. 2014
C4	255	465	0.983	Terrestrially humic-like DOM	Shutova et al., 2014
C5	220	290	0.944	A combination of protein- and tannin-like matter	D'Andrilli et al. 2017
C6	230	355	0.967	Humic-and tryptophan -like DOM	Jörgensen et al. 2011

744

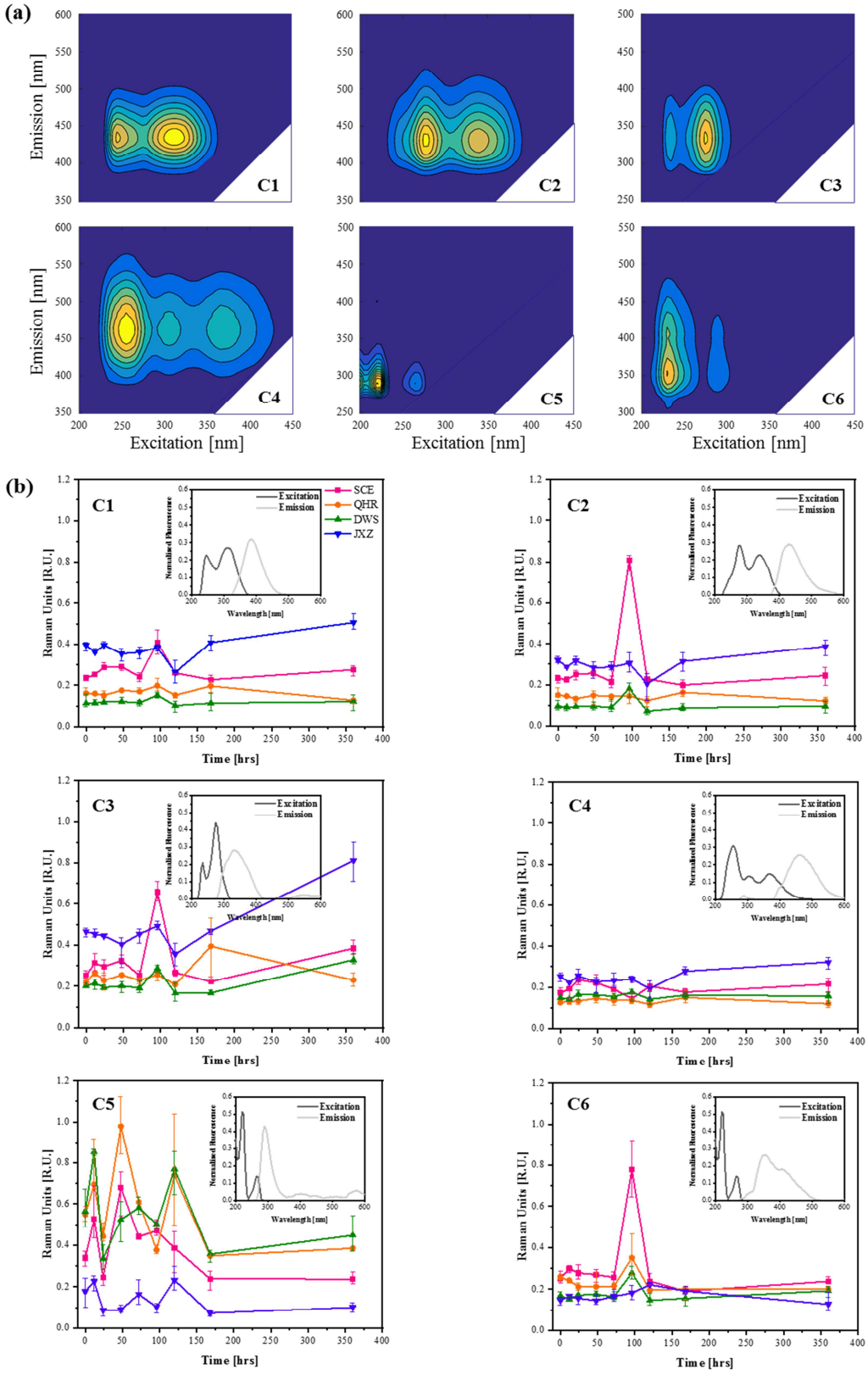

Figure 1. Spectra of the six main components determined via PARAFAC analysis (a) and fluorescent intensities of components (b). (a) EEMs collected from the beginning

748 to the end of experiment across the three replicates for each treatment (n = 3). (b)
749 Insets visualise the respective spectral properties of the six fluorescent components
750 identified by PARAFAC analysis.
751

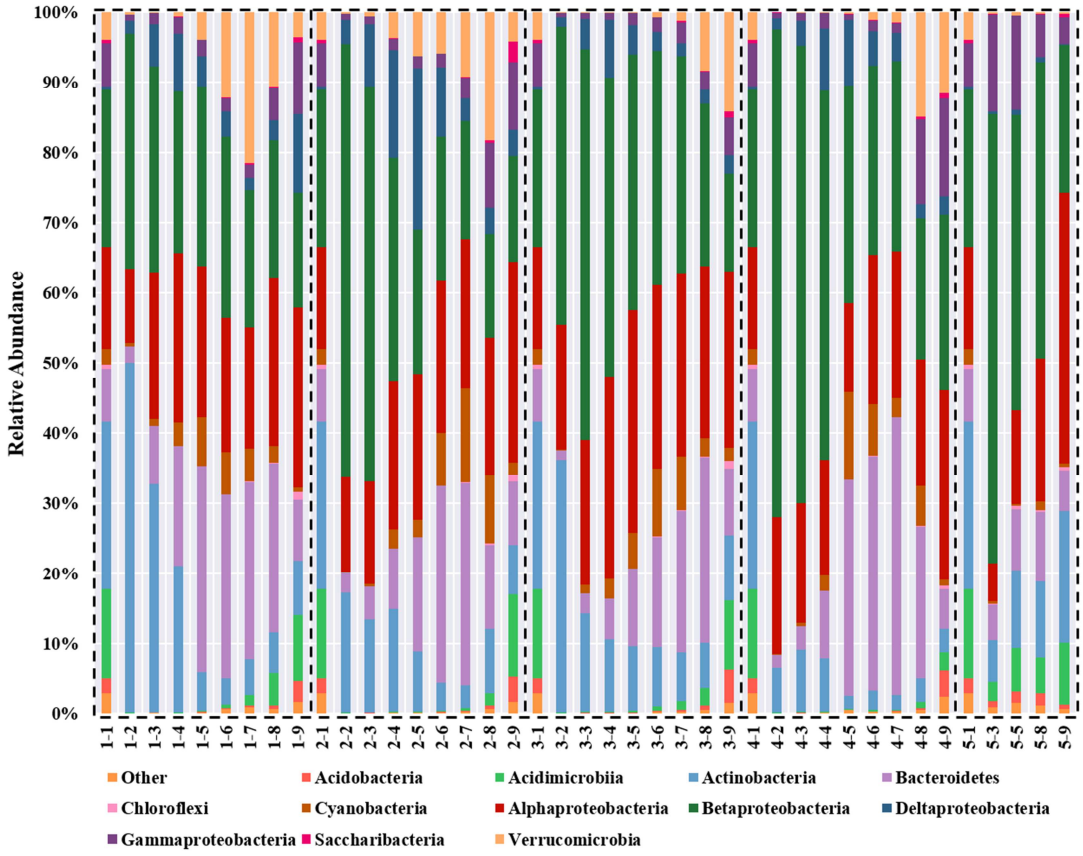

752

753 Figure 2. Taxonomic composition of bacterial experimental communities as relative

754 abundances of each phylum. Proteobacteria and Actinobacteria are identified to class

755 level. 1-1 to 1-9 represent the samples of SCE, 2-1 to 2-9 represent the samples of

756 QHR, 3-1 to 3-9 represent the samples of DWS, 4-1 to 4-9 represent the samples of

757 JXZ, and 5-1 to 5-9 represent the samples of Control.

758

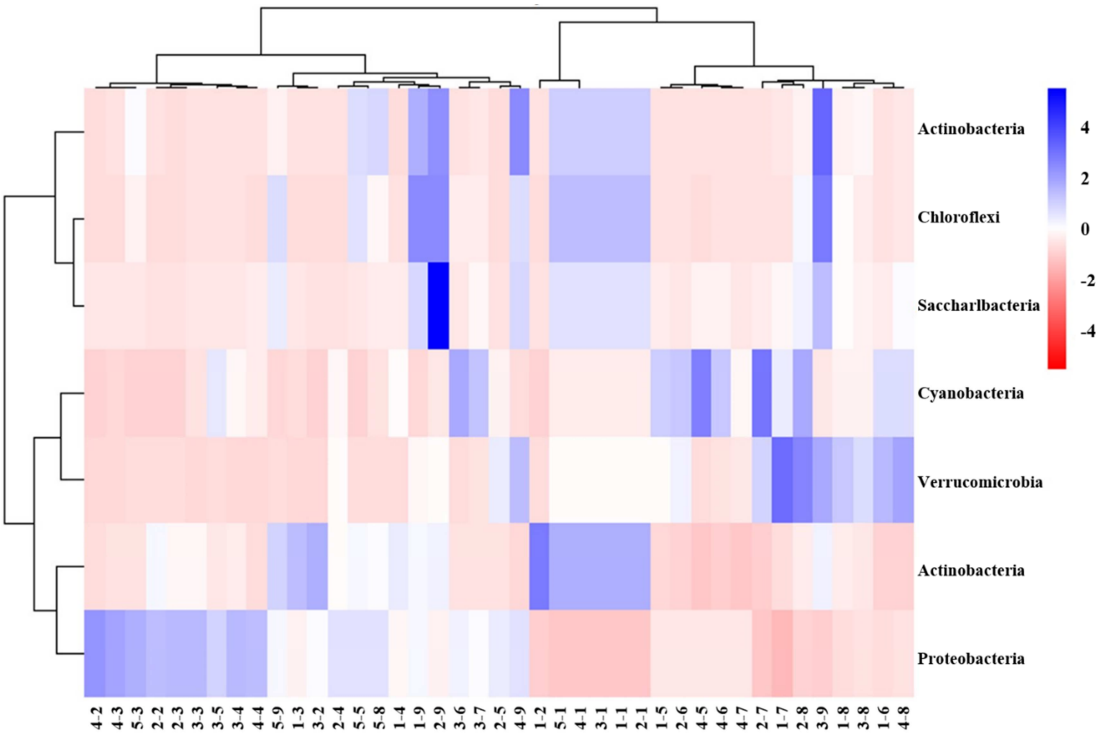

Figure 3. Heatmap showing the taxonomic differences of microbial communities in different treatments based on Bray–Curtis distance. Bray–Curtis distances were calculated using relative abundances of OTUs.

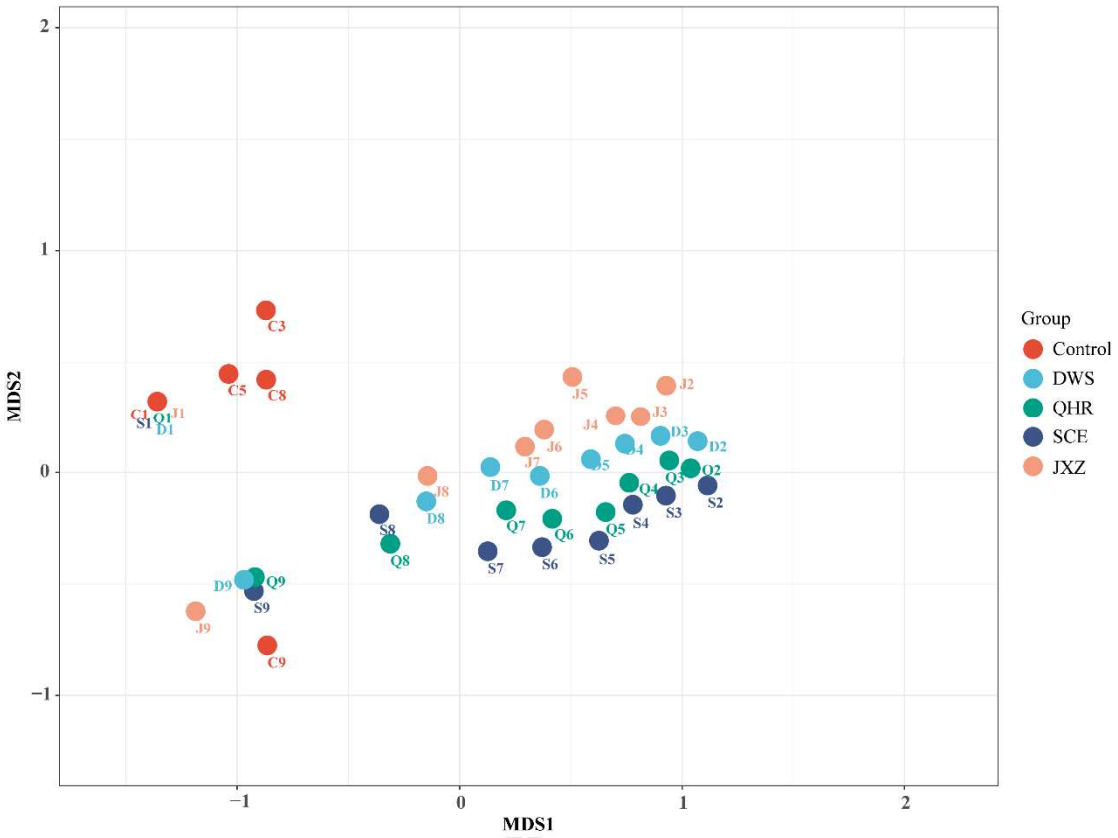

764

765 Figure 4. NMDS representation of bacterial community in five experimental
766 environments. NMDS ordination was derived from pairwise Bray–Curtis distances.
767 S1-S9 represent the microbial community of SCE, Q1-Q9 represent the microbial
768 community of QHR, D1-D9 represent the microbial community of DWS, J1-J9
769 represent the microbial community of JXZ, and C1-C9 represent the microbial
770 community of Control.

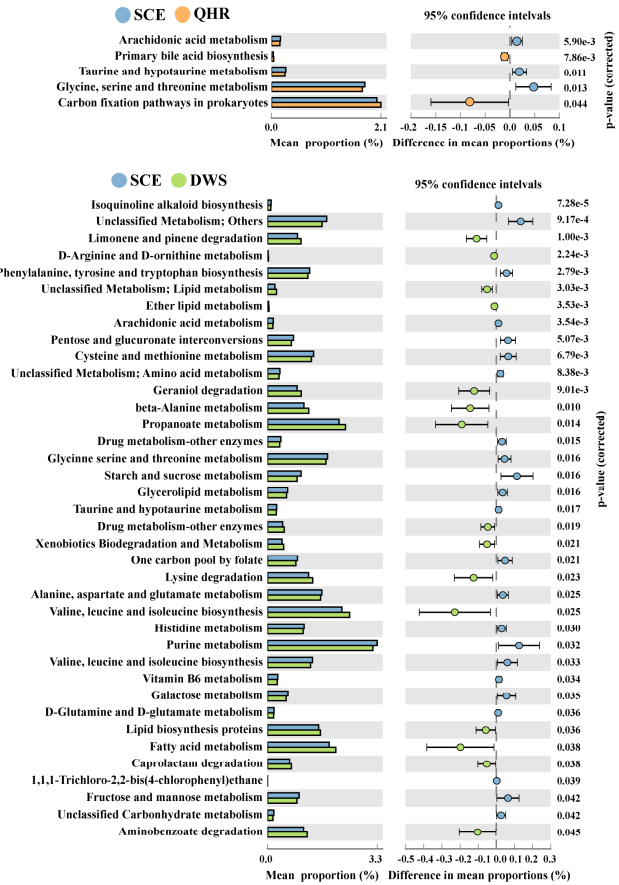
SCE QHR
95% confidence intelvals
Arachidonic acid metabolism
Primary bile acid biosynthesis
Taurine and hypotaurine metabolism
Glycine, serine and threonine metabolism
Carbon fixation pathways in prokaryotes
5.90e-3
7.86e-3
0.011
0.013
0.044
p-value (corrected)
Mean proportion (%)
Difference in mean proportions (%)
SCE DWS
95% confidence intelvals
Isoquinoline alkaloid biosynthesis
Unclassified Metabolism; Others
Limonene and pinene degradation
D-Arginine and D-ornithine metabolism
Phenylalanine, tyrosine and tryptophan biosynthesis
Unclassified Metabolism; Lipid metabolism
Ether lipid metabolism
Arachidonic acid metabolism
Pentose and glucuronate interconversions
Cysteine and methionine metabolism
Unclassified Metabolism; Amino acid metabolism
Geraniol degradation
beta-Alanine metabolism
Propanoate metabolism
Drug metabolism-other enzymes
Glycinne serine and threonine metabolism
Starch and sucrose metabolism
Glycerolipid metabolism
Taurine and hypotaurine metabolism
Drug metabolism-other enzymes
Xenobiotics Biodegradation and Metabolism
One carbon pool by folate
Lysine degradation
Alanine, aspartate and glutamate metabolism
Valine, leucine and isoleucine biosynthesis
Histidine metabolism
Purine metabolism
Valine, leucine and isoleucine biosynthesis
Vitamin B6 metabolism
Galactose metabolism
D-Glutamine and D-glutamate metabolism
Lipid biosynthesis proteins
Fatty acid metabolism
Caprolactam degradation
1,1,1-Trichloro-2,2-bis(4-chlorophenyl)ethane
Fructose and mannose metabolism
Unclassified Carbonhydrate metabolism
Aminobenzoate degradation
7.28e-5
9.17e-4
1.00e-3
2.24e-3
2.79e-3
3.03e-3
3.53e-3
3.54e-3
5.07e-3
6.79e-3
8.38e-3
9.01e-3
0.010
0.014
0.015
0.016
0.016
0.016
0.017
0.019
0.021
0.021
0.023
0.025
0.025
0.030
0.032
0.033
0.034
0.035
0.036
0.036
0.038
0.038
0.039
0.042
0.042
0.045
p-value (corrected)
Mean proportion (%)
Difference in mean proportions (%)

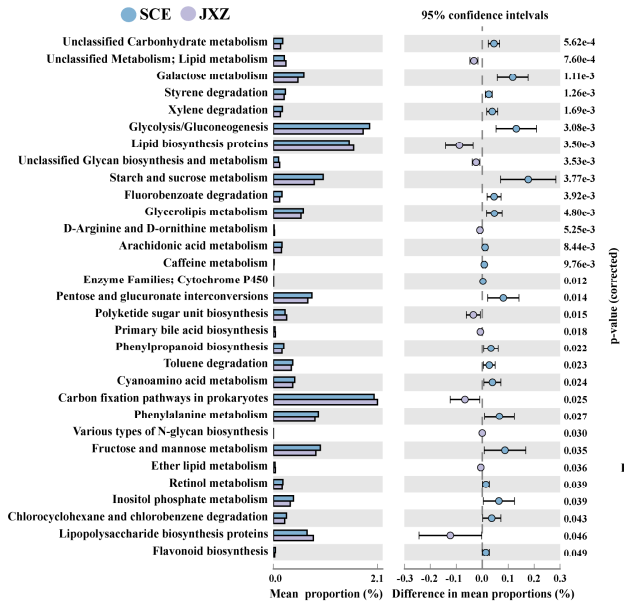
SCE JXZ
95% confidence intelvals
Unclassified Carbonhydrate metabolism
Unclassified Metabolism; Lipid metabolism
Galactose metabolism
Styrene degradation
Xylene degradation
Glycolysis/Gluconeogenesis
Lipid biosynthesis proteins
Unclassified Glycan biosynthesis and metabolism
Starch and sucrose metabolism
Fluorobenzoate degradation
Glycerolipis metabolism
D-Arginine and D-ornithine metabolism
Arachidonic acid metabolism
Caffeine metabolism
Enzyme Families; Cytochrome P450
Pentose and glucuronate interconversions
Polyketide sugar unit biosynthesis
Primary bile acid biosynthesis
Phenylpropanoid biosynthesis
Toluene degradation
Cyanoamino acid metabolism
Carbon fixation pathways in prokaryotes
Phenylalanine metabolism
Various types of N-glycan biosynthesis
Fructose and mannose metabolism
Ether lipid metabolism
Retinol metabolism
Inositol phosphate metabolism
Chlorocyclohexane and chlorobenzene degradation
Lipopolysaccharide biosynthesis proteins
Flavonoid biosynthesis
5.62e-4
7.60e-4
1.11e-3
1.26e-3
1.69e-3
3.08e-3
3.50e-3
3.53e-3
3.77e-3
3.92e-3
4.80e-3
5.25e-3
8.44e-3
9.76e-3
0.012
0.014
0.015
0.018
0.022
0.023
0.024
0.025
0.027
0.030
0.035
0.036
0.039
0.039
0.043
0.046
0.049
p-value (corrected)
Mean proportion (%)
Difference in mean proportions (%)
QHR JXZ
95% confidence intelvals
Glycolysis /Gluconeogenesis
Unclassified Carbohydrate metabolism
Phosphonate and phosphinate metabolism
Lipoic acid metabolism
Inositol phosphate metabolism
Caffeine metabolism
Unclassified Glycan biosynthesis and metabolism
Fluorobenzoate degradation
Galactose metabolism
Citrate cycle (TCA cycle)
D-Arginine and D-ornithine metabolism
Alanine, aspartate and glutamate metabolism
Starch and sucrose metabolism
Unclassified Metabolism;Lipid metabolism
Various types of N-glycan biosynthesis
Fatty acid biosynthesis
Lipid biosynthesis proteins
Ether lipid metabolism
Styrene degradation
Methane metabolism
Retinol metabolism
1.11e-3
2.68e-3
2.70e-3
4.03e-3
4.68e-3
9.04e-3
0.011
0.013
0.021
0.021
0.021
0.025
0.025
0.029
0.033
0.033
0.035
0.039
0.040
0.042
0.050
p-value (corrected)
Mean proportion (%)
Difference in mean proportions (%)

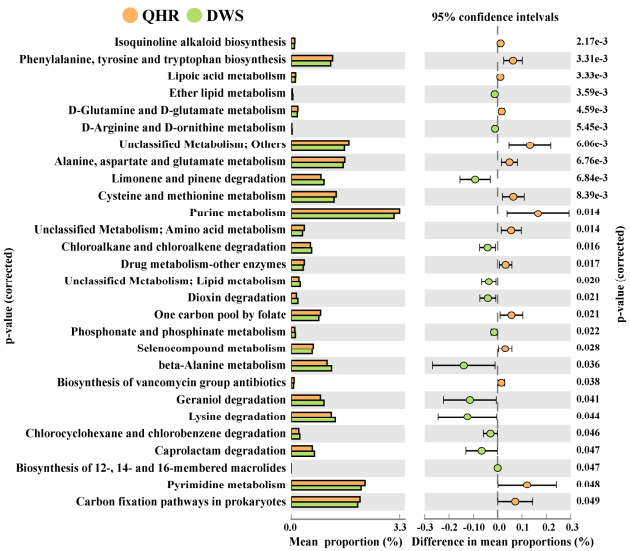
QHR DWS
95% confidence intelvals
Isoquinoline alkaloid biosynthesis
Phenylalanine, tyrosine and tryptophan biosynthesis
Lipoic acid metabolism
Ether lipid metabolism
D-Glutamine and D-glutamate metabolism
D-Arginine and D-ornithine metabolism
Unclassified Metabolism; Others
Alanine, aspartate and glutamate metabolism
Limonene and pinene degradation
Cysteine and methionine metabolism
Purine metabolism
Unclassified Metabolism; Amino acid metabolism
Chloroalkane and chloroalkene degradation
Drug metabolism-other enzymes
Unclassifiecd Metabolism; Lipid metabolism
Dioxin degradation
One carbon pool by folate
Phosphonate and phosphinate metabolism
Selenocompound metabolism
beta-Alanine metabolism
Biosynthesis of vancomycin group antibiotics
Geraniol degradation
Lysine degradation
Chlorocyclohexane and chlorobenzene degradation
Caprolactam degradation
Biosynthesis of 12-, 14- and 16-membered macrolides
Pyrimidine metabolism
Carbon fixation pathways in prokaryotes
2.17e-3
3.31e-3
3.33e-3
3.59e-3
4.59e-3
5.45e-3
6.06e-3
6.76e-3
6.84e-3
8.39e-3
0.014
0.014
0.016
0.017
0.020
0.021
0.021
0.022
0.028
0.036
0.038
0.041
0.044
0.046
0.047
0.047
0.048
0.049
p-value (corrected)
Mean proportion (%)
Difference in mean proportions (%)
DWS JXZ
95% confidence intelvals
Fluorobenzoate degradation
Inositol phosphate metabolism
Isoquinoline alkaloid biosynthesis
Lipopolysaccharide biosynthesis proteins
Lipopolysaccharide biosythesis
Retinol metabolism
Xylene degradation
Carbon fixation pathways in prokaryotes
Chlorocyclohexane and chlorobenzene degradation
Styrene degradation
Polyketide sugar unit biosynthesis
Chloroalkane and chloroalkene degradation
Fatty acid biosynthesis
Linoleic acid metabolism
Cyanoamino acid metabolism
Biosynthesis of vancomycin group antibiotics
Toluene degradation
D-Glutamine and D-glutamate metabolism
Unclassified Metabolism; Amino acid metabolism
Penicillin and cephalosporin biosythesis
Various types of N-glycan biosynthesis
Polycyclic aromatic hydrocarbon degradation
Glycolysis/Gluconeogenesis
Unclassified Metabolism; Others
Caffeine metabolism
Phenylalanine, tyrisine and tryptophan biosynthesis
beta-Lactam resistance
1.32e-3
2.08e-3
2.78e-3
3.43e-3
3.56e-3
3.87e-3
6.03e-3
0.011
0.012
0.013
0.016
0.019
0.022
0.025
0.027
0.029
0.031
0.031
0.034
0.036
0.039
0.040
0.040
0.042
0.042
0.044
0.050
p-value (corrected)
Mean proportion (%)
Difference in mean proportions (%)

771

772 Figure 5. The functional composition of significant changes in intestinal bacterial Kyoto Encyclopedia of Genes and Genomes (KEGG)
773 pathways of level-3 metabolic categories between SCE and QHR, SCE and DWS, SCE and JXZ, QHR and DWS, QHR and JXZ, or DWS and
774 JXZ using the response ratio method at a 95% confidence interval (CI).

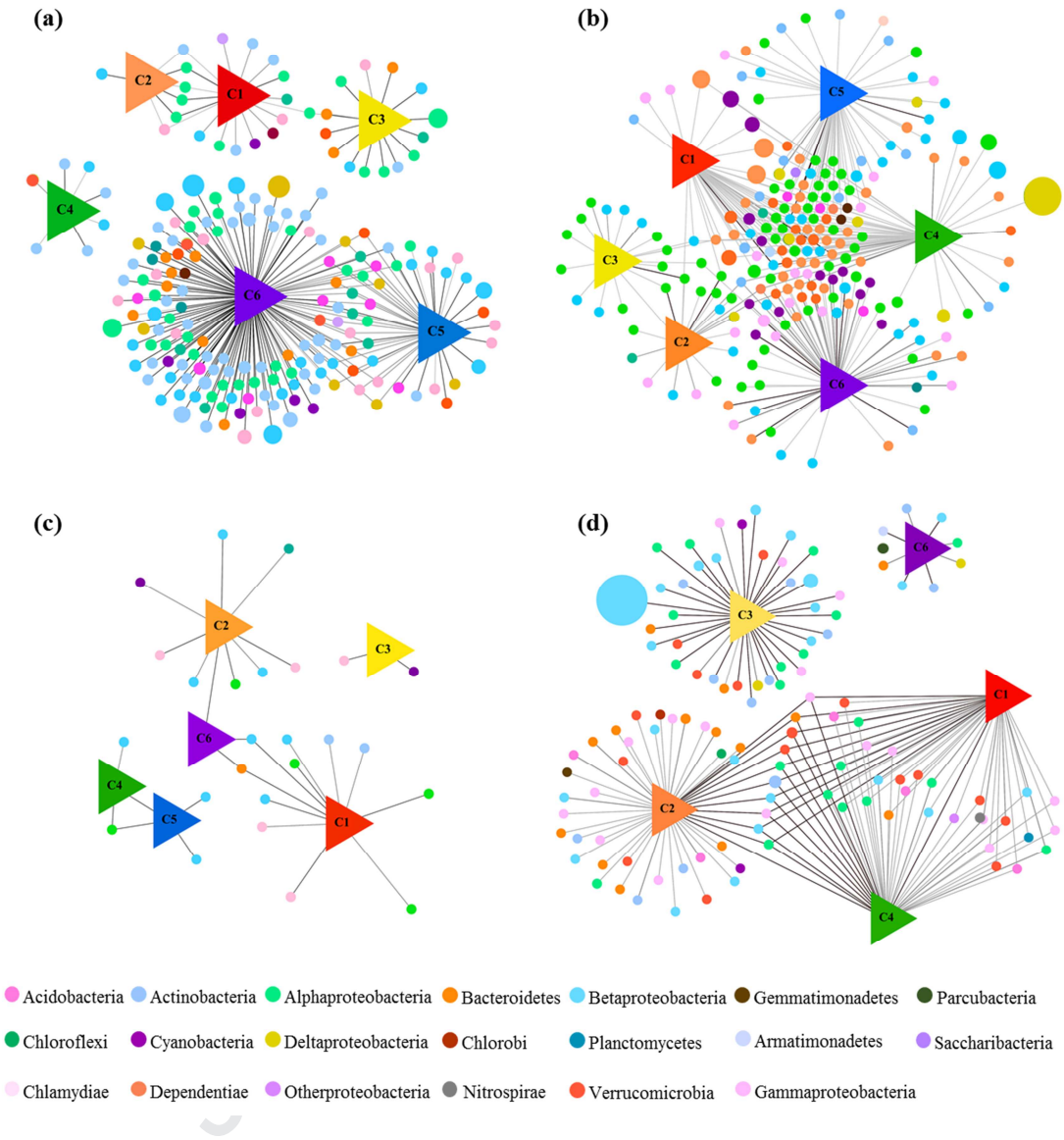

775

776 Figure 6. Associations between DOM components (triangles) and bacterial OTUs
777 (circles) in (a) SCE, (b) QHR, (c) DWS, and (d) JXZ, identified with MIC statistics
778 and visualized as a network. C1-C6 were the DOM components identified by
779 EEM-PARAFAC analysis. The sizes of the circles are proportional to the relative
780 abundance of the OTU.

Highlights

- Proteobacteria showed high connectivity with humic-like DOM.
- *Sphingomonas* were significant at various confluences in urban areas.
- Humic-like -DOM converge could induce a more active lipid metabolism.
- The Carbon metabolism was active when rivers joined with estuary or source water.

Declaration of interests

☒ The authors declare that they have no known competing financial interests or personal relationships that could have appeared to influence the work reported in this paper.

☐The authors declare the following financial interests/personal relationships which may be considered as potential competing interests: